测绘出版社 SURVEYING AND MAPPING PRESS

An Improved Extreme Learning Machine Prediction Model for Ionospheric Total Electron Content

Jianmin WANG, Jiapeng HUANG

School of Geomatics, Liaoning Technical University, Fuxin 123000, *China*

Abstract: Earth's ionosphere is an important medium for navigation, communication, and radio wave transmission. Total Electron Content (TEC) is a descriptive quantify for ionospheric research. However, the traditional empirical model could not fully consider the changes of TEC time series, the prediction accuracy level of TEC data performed not high. In this study, an improved Extreme Learning Machine (ELM) model is proposed for ionospheric TEC prediction. Improvements involved the use of Empirical Mode Decomposition (EMD) and a Fuzzy C-Means (FCM) clustering algorithm to pre-process data used as input to the ELM model. The proposed model fully uses the TEC data characteristics and expected to perform better prediction accuracy. TEC measurements provided by the Centre for Orbit Determination in Europe (CODE) were used to evaluate the performance of the improved ELM model in terms of prediction accuracy, applicable latitude, and the number of required training samples. Experimental results produced a Mean Relative Error (MRE) and a Root Mean Square Error (RMSE) of 8.5% and 1.39 TECU, respectively, outperforming the ELM algorithm (RMSE = 2.33 TECU and MRE = 17.1%). The improved ELM model exhibited particularly high prediction accuracy in mid-latitude regions, with a mean relative error of 7.6%. This value improved further as the number of available training data increased and when 20-doys data were trained, achieving a mean relative error of 4.9%. These results suggest the proposed model offers higher prediction accuracy than conventional algorithms.

Key words: ELM model; EMD; FCM; incentive function; ionospheric TEC prediction

Citation: Jianmin WANG, Jiapeng HUANG. An Improved Extreme Learning Machine Prediction Model for Ionospheric Total Electron Content[J]. Journal of Geodesy and Geoinformation Science, 2023, 6(1): 1-10. DOI: 10.11947/j.JGGS.2023.0101.

1 Introduction

TEC is the total number of electrons measured at the intersection of a cylinder of the Earth's ionosphere and the cylinder with a 1 square meter base area of the atmosphere along the signal path occurring between the Global Navigation Satellite Systems (GNSS) satellite and the GNSS receiver on the earth[1-3]. Ionospheric TEC was first proposed by scholars in the 1960s and is measured in TEC Units (TECU), where 1 TECU = 10^{16} electrons/m^2[4-6]. Existing TEC prediction research primarily consists of studies on ionospheric variational characteristics[7]. Applications have been reported for navigation and positioning[8], investigating factors influencing ionospheric conditions[9-12], and earthquake prediction[13-15]. TEC values could also cause delays in GNSS signals and reduce the accuracy of estimated positions. As such, the prediction of TEC is critical for ionospheric studies[16-17].

Research in ionospheric TEC modeling has focused primarily on improving prediction accuracy. For example, Jakobsen et al.[18] used Singular Value Decomposition (SVD) to analyze a TEC time series over nine years, using a robust dataset calculated by Kalman filtering. The authors determined time-varying characteristics for the ionosphere and predicted a future annual model. An et al.[19] divided ionospheric TEC into a trend term and a non-trend term. The authors then used a Fourier triangle series and

Received date: 2022-01-11; accepted date: 2022-03-21
Foundation support: National Natural Science Foundation of China (No. 41474020)
First author: Jianmin WANG, associate professor, majors in GNSS data processing.
E-mail: wjminlntu@163.com
Corresponding author: Jiapeng HUANG, associate professor, majors in GNSS and LiDAR data processing.
E-mail: 18941821626@163.com

an Auto Regressive and Moving Average (ARMA) model to predict the trend and non-trend terms, respectively. These terms were then used to reconstruct the final predicted TEC values. Experimental results showed that a combination of these two models was effective for TEC prediction over a large range using only a few parameters. Liu et al.[20] combined wavelet analysis with an Auto Regressive Integrated Moving Average (ARIMA) model to develop the WARIMA model. Experiments showed this combined approach outperformed the single ARIMA algorithm.

Lu et al.[21] combined SVD with ARMA to decompose an ionospheric TEC time series and forecast components. Results demonstrated that the prediction accuracy of a single model was improved by including SVD. However, there was no considerable improvement in accuracy for small numbers of components, while large collections suffered from the presence of cumulative errors that led to a decline in consistency. Tang et al.[22] decomposed an ionospheric TEC time series using Empirical Mode Decomposition (EMD). This approach utilized ionospheric TEC grid data published by the International GNSS Service (IGS) at varying times and locations. The prediction of each decomposed series was conducted using the ARMA model. Experimental results showed an increase in relative prediction accuracy compared with single time series models. Each of the techniques discussed above improved TEC prediction accuracy using pre-processing steps.

Wang et al.[23] organically combined a Genetic Algorithm (GA) with a Neural Network (NN) to optimize the initial weights used by the GA, in order to avoid the local minimum problem that often occurs during NN training. Results demonstrated that this hybrid GA-NN algorithm offered high accuracy and reliability in predicting ionospheric TEC. The model also outperformed the basic NN and the International Reference Ionosphere (IRI) model. Liu et al.[24] introduced a Wavelet Neural Network (WNN) for ionospheric TEC prediction and used ionospheric TEC information released by IGS as experimental data. Results indicated that this combined model with pre-processing achieved high short-term prediction accuracy.

Cesaroni et al.[25] developed a model to forecast TEC values, the Middle East Technical University neural network (METU-NN) model. The METU-NN is a data-driven neural network consisting of one hidden layer and several neurons. Acharya et al.[26] used an adaptive recurrent neural network and an in-situ learning algorithm to predict TEC in non-anomalous areas. Wang et al. improved on the single NN prediction model by weighting and pre-processing the data[27-28]. Results indicated the optimized model offered better prediction performance than the single NN. Huang et al.[29] used TEC data from four GNSS reference stations (BJFS, XIAN, WUHN, and KUNM—from 2007 to 2011) to improve a back-propagation NN prediction model using a GA. Results showed the improved model to be highly reliable. Sabzehee et al.[30] demonstrated that regional ionospheric modeling using an artificial neural network (ANN) is a viable technique for predicting TEC at both single- and double-frequency GPS receivers. The ANN demonstrated acceptable capability and flexibility in modeling and predicting TEC values. Tebabal et al.[31] developed a neural network-based regional ionospheric model using GPS-TEC data from Eastern Africa. Inyurt et al.[32] modeled and predicted seasonal ionospheric TEC using an ANN. The model produced more accurate predictions in winter and autumn than in summer or spring, with RMSE and TEC values of 3.92 and 3.97, respectively.

Previous studies have also shown that EMD can improve the performance of forecasting models[22]. In addition, neural network-based prediction performed better than time series modeling. Further study of the EMD algorithm suggests the Intrinsic Mode Function (IMF) suffers from issues such as aliasing that can decrease the accuracy of the prediction model[22]. The use of Fuzzy C-Means (FCM) clustering was proposed after EMD to reduce the impact of aliasing. Each group of IMF functions was pre-processed by FCM clustering and the resulting data were used to train the NN model.

Extreme Learning Machine (ELM) models have achieved high prediction accuracy in multiple

fields. However, the number of hidden layer neurons and the incentive function used by the algorithm may reduce its prediction accuracy if not sufficiently optimized[33]. As a result, empirical models are often used for such predictions though they are not applicable in all situations. As such, in this paper, we propose an improved ELM model that selects a specific number of hidden layer neurons and the excitation function to be used in a NN. We selected the optimal neural network model by traversing the number of all neurons. An ionospheric TEC time series is first acquired and is then decomposed using the EMD algorithm. Decomposed IMF functions are clustered and are then pre-processed using the FCM algorithm. Finally, the ELM model (with an optimal number of hidden layer neurons and a pre-selected excitation function) is used to predict a TEC time series. The proposed model fully excavates the TEC data characteristics and expects to perform better prediction accuracy. This study focuses on evaluating the prediction accuracy, latitude dependence, and training sample length sensitivity for the improved ELM model.

2 Data and Methods

2.1 The empirical mode decomposition algorithm

Ionospheric TEC data consist of time series with non-stationary and non-linear characteristics. As such, it is difficult to describe the corresponding signal features using traditional analysis. However, the EMD method provides a reasonable definition for instantaneous frequency and can therefore describe the physical meaning of a TEC time series[34-38]. The data $x(t)$ decomposed by the EMD algorithm can be represented as follows

$$x(t) = \sum_{i=1}^{n} c_i(t) + r_n(t) \tag{1}$$

where $c_i(t)$ is the IMF component of different TEC data groups and $r_n(t)$ is a trend term for the TEC data, representing the average signal near a linear mode trend.

2.2 The fuzzy C-means clustering algorithm

A direct use of IMF component data (decomposed by the EMD algorithm) can lead to several issues, such as the prediction model requiring increasing input variables or correlations occurring between the input and time series data. These effects can reduce the operational efficiency and generalizability of the prediction model. To resolve these issues, an FCM algorithm was introduced into the combination model for dimension-reducing clustering, used for ionospheric TEC data preprocessing[39-41]. This FCM algorithm calculates the membership degree of each variable and cluster center, respectively expressed as follows[42-44]

$$\mu_{ij}^{(t)} = \left\{ \sum_{k=1}^{c} \left[\left(\frac{d^{(t)}(x_i, z_j)}{d^{(t)}(x_i, z_k)} \right)^{\frac{2}{m-1}} \right] \right\}^{-1}, \quad i = 1, 2, \cdots, n \tag{2}$$

$$z_j^{(t+1)} = \frac{\sum_{i=1}^{n} (\mu_{ij}^{(t+1)})^m \cdot x_i}{\sum_{i=1}^{n} (\mu_{ij}^{(t+1)})^m}, \quad i = 1, 2, \cdots, n \tag{3}$$

where $\| \cdot \|$ is a suitable matrix norm. When $\| z(t+1) - z(t) \| < \zeta$, $\zeta < 0.01$ and the clustering is considered to be complete as the center converges.

2.3 The ionospheric TEC prediction model

Conventional Neural Network (CNN) algorithms use empirical methods to select learning rates appropriate for experimental data and to prevent the network from over-training and converging to a local minimum. In contrast, the ELM model only re-quires the number of neurons in the hidden layer to be specified. In this study, the ELM model with added pretreatment was applied to TEC prediction for the first time. During the training process, the model randomly selects input parameters in the hidden layer and determines output parameters by solving for the Moore-Penrose generalized inverse of the output matrix in the hidden layer. This approach significantly increases training speed with better generalizability than that of CNNs. As such, the ELM model is widely used in traffic flow[45], short-term wind speed[46], and food-price forecasting[47]. In this paper, an improved ELM model with pretreatment is applied to ionospheric TEC prediction.

An appropriate excitation function and neuron quantity are the primary factors affecting ELM model

performance. Accurate prediction results require optimized neuron counts in the hidden layer and specific types of excitation functions. These parameters can be chosen by comparing the prediction errors obtained with different network architectures in this paper.

(1) Neuron quantities in the hidden layer.

The number of neurons in the hidden layer is closely correlated with model prediction accuracy, which can be improved by optimizing the neuron count for specific experimental data. However, model complexity also increases with neuron quantity and excessive complexity can increase runtimes and even reduce prediction accuracy. As such, determining the optimal number of neurons is an important factor affecting model performance. A variety of neuron selection techniques have been proposed in the literature, including pruning, growth, evolutionary, and adaptive methods. In this study, the optimal number of neurons was determined by traversing over a range from 1 to 30. In the prediction experiments in the study, the method was used to establish the optimization model. This approach was used because of the fast convergence characteristics of the ELM model.

(2) The excitation function.

Differing excitation functions provide varying predictive performance, based on the type of experimental data. In this study, experiments were conducted by selecting different numbers of hidden layer neurons for each tested excitation function. The optimal function and the ideal number of hidden layer neurons were selected based on the prediction results produced by each test. A list of excitation functions used in this study is provided in Tab.1. A flowchart for this proposed technique is shown in Fig.1.

Tab.1 Various excitation functions

Function name	Functional expression
Bent	$f(x)=\frac{\sqrt{x^2+1}-1}{2}+x$
PReLU	$f(x)=\begin{cases}0, & x<0\\ \alpha x, & x\geqslant 0\end{cases}$
SoftPlus	$f(x)=\ln(1+e^x)$
ELU	$f(x)=\begin{cases}0, & x<0\\ \alpha(e^x-1), & x\geqslant 0\end{cases}$
Sinc	$f(x)=\begin{cases}\frac{\sin(x)}{x}, & x=0\\ 1, & x\neq 0\end{cases}$
Gaussian	$f(x)=e^{-x^2}$
Tanh	$f(x)=2\mathrm{Sigmoid}(2x)-1$
Hardlim	$f(x)=\begin{cases}1, & x<0\\ 0, & x=0\\ 1, & x>0\end{cases}$
Sine	$f(x)=\sin(x)$
Sigmoid	$f(x)=\frac{1}{1+e^{-x}}$

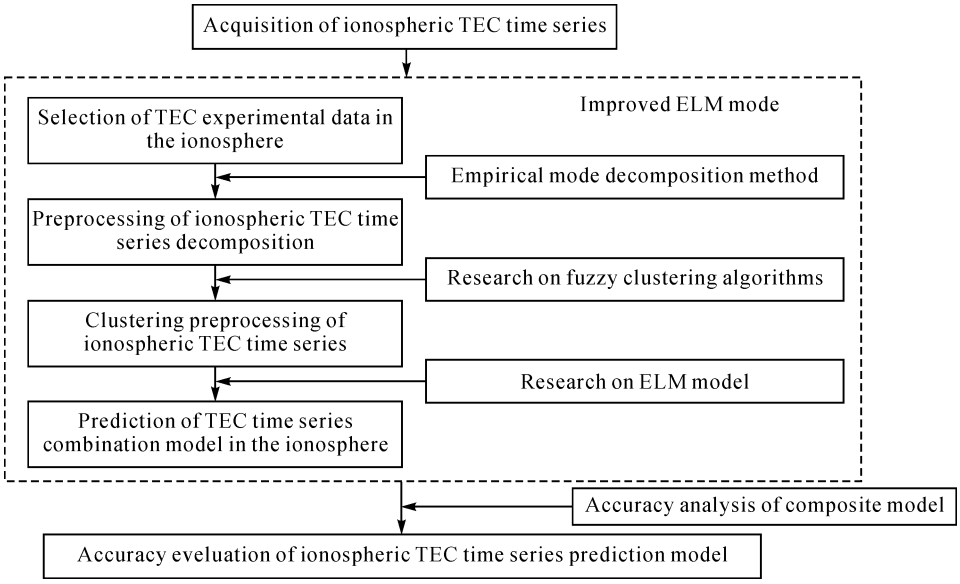

Fig.1 A flowchart of the improved Extreme Learning Machine (ELM) model

2.4 Study data

The proposed ELM algorithm was compared with the Auto Regressive (AR), Non-linear Auto-Regressive (NAR), and first-order single variable grey (GM(1, 1)) models, which were applied to the same experimental data from the Centre for Orbit Determination in Europe (CODE). Prediction accuracy was evaluated using the metrics discussed previously and a series of experiments were conducted using nine sets of TEC data involving varying latitude conditions. Model performance was also assessed for different training data quantities using three groups consisting of 10-doys, 5-doys, and 20-doys data used to backward-predict 1-doy conditions. For example, take 10 doys as training data and predict 1 doy backward. In order to use 101—110 doys as training data and 111 doy as predicting data. Information relevant to each experimental group is provided in Tab.2.

Tab.2 Study data and experimental conditions

Grid point information		Year	Latitude	Training data/doy
Experimental group 1	Experiment 1	2008	(125°W, 87.5°N)	51—60
	Experiment 2	2011	(125°W, 45°N)	101—110
	Experiment 3	2014	(125°W, 22.5°N)	201—210
Experimental group 2	Experiment 4	2007	(125°W, 22.5°S)	31—35
	Experiment 5	2009	(125°W, 45°S)	151—155
	Experiment 6	2006	(125°W, 87.5°S)	351—355
Experimental group 3	Experiment 7	2017	(15°E, 45°N)	21—40
	Experiment 8	2017	(65°E, 45°N)	21—40
	Experiment 9	2017	(125°E, 22.5°S)	21—40

2.5 Evaluation of accuracy

A series of metrics were used to evaluate the prediction accuracy of the improved ELM model and demonstrate its superior performance compared to conventional techniques. These included the Mean Relative Error (MRE), Mean Square Error (MSE), Root Mean Square Error (RMSE), and Mean Absolute Error (MAE), respectively defined as follows

$$\mathrm{MRE}=\frac{1}{n}\sum_{i=1}^{n}\frac{|\hat{x}_n-\tilde{x}_n|}{\tilde{x}_n},\quad i=1,2,\cdots,n \tag{4}$$

$$\mathrm{MSE}=\frac{\sum_{i=1}^{n}(\hat{x}_n-\tilde{x}_n)^2}{n},\quad i=1,2,\cdots,n \tag{5}$$

$$\mathrm{RMSE}=\frac{\sqrt{\sum_{i=1}^{n}(\hat{x}_n-\tilde{x}_n)^2}}{n},\quad i=1,2,\cdots,n \tag{6}$$

$$\mathrm{MAE}=\frac{\sum_{i=1}^{n}|\hat{x}_n-\tilde{x}_n|}{n},\quad i=1,2,\cdots,n \tag{7}$$

In these expressions, $\hat{x}_n$ is the predicted result, $\tilde{x}_n$ is the actual CODE data, and n is the number of data samples.

3 Results and Analysis

The prediction accuracy of the proposed ELM model was compared with conventional forecasting models under different experimental conditions. Results using various data groups are shown in Fig. 2 and Tab.3, with results from nine experiments for different models shown in Tab.4.

Tab.3 Accuracy results for the improved ELM model

Experiment	RMSE/TECU	MRE/(%)	MAE/TECU	MSE/TECU	Excitation function	The number of hidden layers
1	0.566	14.0	0.435	0.320	ELU	21
2	1.408	7.4	1.071	1.983	Sig	10
3	1.198	3.3	0.875	1.434	Bent	7
4	5.992	15.4	3.598	35.905	ELU	2
5	1.023	13.2	0.868	1.046	SoftPlus	21
6	0.645	8	0.56	0.416	Gaussian	6
7	0.429	3.7	0.299	0.184	ELU	5
8	0.588	6.2	0.487	0.346	Bent	21
9	0.639	4.9	0.55	0.409	Tanh	23

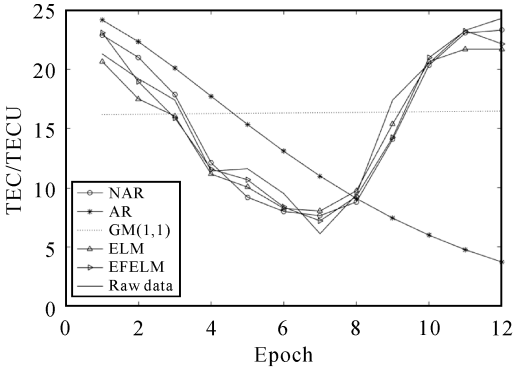

(a) Results from a study site located at 125° W and 45° N (Data collected from 101—110 doys of 2011 were included in the training set. Forecasted 111 doy (see Experiment 2))

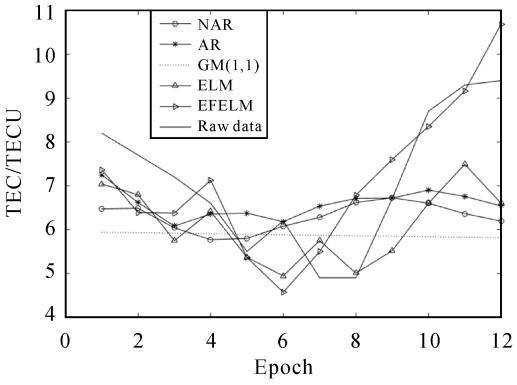

(b) Results from a study site located at 125° W and 45° S (Data collected from 151—155 doys of 2009 were included in the training set. Forecasted 156 doy (see Experiment 5))

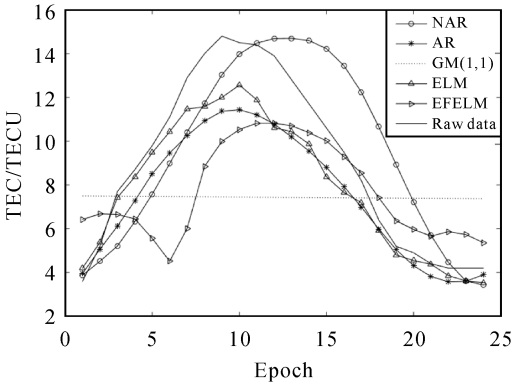

(c) Results from a study site located at 65°E and 45°N (Data collected from 21—40 doys of 2017 were included in the training set. Forecasted 41 doy (see Experiment 8))

Fig.2 Predict results

Fig. 2 demonstrates that the improved ELM model is closer to the original data than other models. The NAR model produced an MRE of 32.2% and an RMSE of 3.97 TECU. The AR model produced an MRE of 26.7% and an RMSE of 3.49 TECU. GM(1,1) produced an MRE of 40.9% and an RMSE of 5.02 TECU. The ELM model produced an MRE of 17.1% and an RMSE of 2.33 TECU. The best performance was achieved by the improved ELM model with an MRE of 8.5% and an RMSE of 1.39 TECU.

As shown in Tab.3, the accuracy evaluation indexes of Experiment 2 and Experiment 4 were reduced. Observing the two groups of experimental data, it can be seen that there are abnormal TEC data in the two groups of data. Considering the abnormal situation of TEC data, this may be the main reason for the lower accuracy evaluation index of prediction model. Although the accuracy evaluation index decreased in Experiment 2 and Experiment 4, the proposed model showed high accuracy evaluation index in other groups of experiments. Summarizing the experimental data of all groups, it can be seen that the accuracy evaluation index of the proposed ELM prediction model performed at a good level. It is a positive phenomenon, which proves the superiority of proposed TEC prediction model. Limited by the length of the paper, we only select 9 grid points in the world as experimental data to evaluate the accuracy of TEC data prediction model. In order to further verify the accuracy of our proposed prediction model, we will promote the proposed prediction model globally in future research and further evaluate the prediction ability of our proposed model.

The short-term TEC prediction of ionosphere based on ARIMA model in Literature [7] achieved MRE = 14% ~ 17%. An improved TEC forecast of short-term ionosphere based on wavelet-ARIMA in Literature [13] achieved MRE = 10% ~ 15%. As a comparison, it can be found that the improved algorithm proposed in Literature [13] performed better accuracy evaluation index than the original ARIMA algorithm in Literature [7]. Moreover, the proposed algorithm performed higher accuracy evaluation index than that in Literature [7] and traditional ELM model (RMSE = 2.33 TECU, MRE = 17.1%). Compared with the experimental results, the proposed preprocessing algorithm may improve the prediction ability of the model for TEC data more than the original algorithm. Although the characteristics of TEC data are low regularity and high uncertainty, EMD algorithm combined with FCM algorithm may increase the model's understanding of TEC data and

improve the prediction accuracy of the model. The experimental results also show that the preprocessing may be used as a new way to improve the prediction accuracy of TEC data prediction model.

These results indicate the improved ELM algorithm to be the most accurate as it is able to adjust parameters for differing types of ionospheric TEC data. As a result, the model can be applied broadly and yet maintain high prediction accuracy. This also suggests that if a group of experimental data results in low accuracy, it will affect the prediction metrics of the model. However, the proposed ELM algorithm offers stable performance and can maintain high prediction accuracy across experiments and data types. Experimental results also showed that the addition of decomposition clustering during pre-processing improved the model's ability to effectively utilize training samples and further improved its forecasting capabilities (Tab.4).

Tab.4 Average accuracy results for different models

Model name	RMSE /TECU	MRE /(%)	MAE /TECU	MSE /TECU
NAR	3.97	32.2	3.38	40.15
AR	3.49	26.7	2.93	22.51
GM(1,1)	5.02	40.9	4.35	38.62
ELM	2.33	17.1	1.77	8.73
Improved ELM	1.39	8.5	0.97	4.67

4 Discussion

4.1 Prediction experiments at different latitudes

Experiments were conducted using data from high (87.5°), mid (45°), and low (22.5°) latitudes, as shown in Tab.5.

Tab.5 Improved ELM results at various latitudes

Sample latitude	RMSE /TECU	MRE /(%)	MAE /TECU	MSE /TECU
High	0.61	11.0	0.50	0.37
Mid	0.86	7.6	0.68	0.89
Low	2.61	7.9	1.67	12.58

The consistency of these metrics demonstrates the accuracy of the improved ELM model in different regions. The MRE in Tab.5 reached 11.0%, 7.6%, and 7.9% for high, mid, and low latitudes, respectively. The improved ELM model also exhibited the smallest error at high latitudes among the algorithms tested. Actual TEC values showed variations ranging from 10 TECU (high lat.) to 40 TECU (low lat.) in different sampling areas. By comparing the experimental data and error metrics, it is evident that MRE values were lower at low latitudes while other error metrics were lower at high latitudes. The proposed ELM model generally performed better in mid-latitude regions.

By comparing the changes of the experimental data, we can find that the data changes are not obvious in the mid-latitude. Moreover, compared with the high latitude and low latitude, the data changes in the middle latitudes have more obvious regularity than high latitude and low latitude, which can be more easily found by the prediction model, so the model performed better applicability and can obtain the evaluation index showing higher prediction accuracy. And, the research adds a preprocessing method before the prediction model, so that the model has higher adaptability to the research data than the direct processing data.

4.2 Prediction experiment with training samples of different lengths

Experiments were conducted using training samples of different lengths, as shown in Tab.6.

Tab.6 Prediction results with training samples of different lengths

Length /doys	RMSE /TECU	MRE /(%)	MAE /TECU	MSE /TECU
5	2.55	12.2	1.68	12.46
10	1.06	8.2	0.79	1.25
20	0.55	4.9	0.45	0.31

Experiments utilizing training samples of varying lengths were conducted to study its influence on ELM accuracy. The MRE values for training sample lengths of 5, 10, and 20 doys were 12.2%, 8.2%, and 4.9%, respectively. An analysis of other error metrics indicated that prediction accuracy for the improved ELM model increased gradually with the number of training samples, with 20-doys data providing the best results. As such, the accuracy of the

proposed model could be further improved by increasing the number of training samples.

The training data length of 20 doys performed better. A possible reason is that the proposed model with training data more fully adapts to the research data than 5 and 10 doys. If there are special situations such as the magnetic storm in the training length, it will seriously affect the applicability of the model, while the 20-doys training length reduces the impact of special situations such as the magnetic storm on the model and made the adaptability of the model perform better than 5 and 10 doys. Therefore, the 20-doys training data length shows the optimal prediction accuracy in the experiment. However, the longer the training data will not produce better prediction accuracy, and we will focus on the optimal training data length in the future research.

5 Conclusion and Prospect

An improved ELM model based on empirical mode decomposition and a fuzzy C-means algorithm was presented in this study, to increase prediction accuracy for ionospheric TEC data. The proposed model decomposed experimental data and acquired different IMF data groups. A fuzzy C-means algorithm was then utilized to complete the clustering of IMF data, which were input to the ELM model. A series of experiments were conducted to evaluate prediction performance, from which the following conclusions were drawn:

(1) MRE and RMSE for the improved ELM model were 8.5% and 1.39 TECU, respectively. The improved ELM algorithm (RMSE = 1.39 and MRE = 8.5%) exhibited higher prediction accuracy than the ELM algorithm (RMSE = 2.33 and MRE = 17.1%).

(2) Multiple experimental groups were used to study the applicability of the proposed model at different latitudes. Results from varying sample regions showed that the improved ELM model had a high prediction accuracy for mid-latitude data, with an MRE of 7.6%.

(3) The effect of training data length on model performance was also investigated. It was observed that prediction accuracy improved as the length of training data increased. The best performance was achieved when 20-doys data were used to predict 1-doy ahead, exhibiting an MRE of 4.9%.

The proposed model offers several advantages over conventional algorithms such as NAR. Improved forecasting performance allows the model to be extended to global ionospheric grid prediction research. In the follow-up study, we will explore the impact of magnetic storms on TEC data model.

References

[1] CANDER L R, HARALAMBOUS H. On the importance of total electron content enhancements during the extreme solar minimum[J]. Advances in Space Research, 2011, 47(2): 304-311.

[2] CANDERL R. Re-visit of ionosphere storm morphology with TEC data in the current solar cycle[J]. Journal of Atmospheric and Solar-Terrestrial Physics, 2016, 138-139: 187-205.

[3] HABARULEMA J B, KATAMZI Z T, SIBANDA P, et al. Assessing ionospheric response during some strong storms in solar cycle 24 using various data sources[J]. Journal of Geophysical Research: Space Physics, 2017, 122(1): 1064-1082.

[4] NAVA B, COÏSSON P, RADICELLA S M. A new version of the NeQuick ionosphere electron density model[J]. Journal of Atmospheric and Solar-Terrestrial Physics, 2008, 70(15): 1856-1862.

[5] JAKOWSKI N, HOQUE M M, MAYER C. A new global TEC model for estimating transionospheric radio wave propagation errors[J]. Journal of Geodesy, 2011, 85(12): 965-974.

[6] TANG Jun. Studies on three-dimension ionospheric tomography using GNSS measurements and ionospheric disturbances[J]. Acta Geodaetica et Cartographica Sinica, 2015, 44(1): 117. DOI:10.11947/j.AGCS.2015.20130398.

[7] ZHANG Xiaohong, REN Xiaodong, WU Fengbo, et al. Short-term TEC prediction of ionosphere based on ARIMA model [J]. Acta Geodaetica et Cartographica Sinica, 2014, 43(2): 118-124. DOI:10.13485/j.cnki.11-2089.2014.0018.

[8] WANG Jianmin, LI Yabo, MA Tianming, et al. Real time and fast algorithm for integer ambiguity of reference stations in large-scale network RTK[J]. Bulletin of Surveying and Mapping, 2017 (10): 7-11. DOI: 10.13474/j.cnki.11-2246.2017.0307.

[9] DENG Zhongxin, LIU Ruiyuan, ZHEN Weimin, et al. Study on the ionospheric TEC storms over China [J]. Chinese Journal of Geophysics, 2012, 55(7): 2177-2184.

[10] SHARMA G, RAY P, MOHANTY S, et al. Ionospheric TEC modelling for earthquakes precursors from GNSS data [J]. Quaternary International, 2017, 462: 65-74.

[11] CHERNOUSSA, SHAGIMURATOVII, IEVENKOIB, et al. Auroral perturbations as an indicator of ionosphere impact on

navigation signals[J]. Russian Journal of Physical Chemistry B,2018, 12(3):562-567.

[12] MUKESHR, KARTHIKEYANV, SOMAP,et al. Cokriging based statistical approximation model for forecasting ionospheric VTEC during high solar activity and storm days[J]. Astrophysics and Space Science,2019, 364(8):131.

[13] LIU Xiandong, SONG Lijie, YANG Xiaohui, et al. Predicting shortdated ionospheric TEC based on wavelet neural network [J]. Hydrographic Surveying and Charting, 2010, 30(5): 49-51, 55.

[14] AKHOONDZADEH M, DE SANTIS A, MARCHETTI D, et al. Anomalous seismo-LAI variations potentially associated with the 2017 M_W = 7.3 Sarpol-e Zahab (Iran) earthquake from swarm satellites, GPS-TEC and climatological data[J]. Advances in Space Research, 2019, 64(1): 143-158.

[15] YAN Xiangxiang, SHAN Xinjian, CAO Jinbin, et al. Preliminary study of the seimoionospheric perturbation before Tohoku-oki M_W 9.0 earthquake[J]. Progress in Geophysics, 2013, 28(1): 155-164.

[16] ZHAO Chuanbao, ZHANG Baocheng, ODOLINSKI R, et al. Combined use of single-frequency data and global ionosphere maps to estimate BDS and Galileo satellite differential code biases[J]. Measurement Science and Technology, 2020, 31 (1): 015002.

[17] PEREZ R O. Using Tensor Flow-based neural network to estimate GNSS single frequency ionospheric delay [J]. Advances in Space Research, 2019, 63(5): 1607-1618.

[18] JAKOBSEN J, KNUDSEN P, JENSEN A B O. Analysis of local ionospheric time varying characteristics with singular value decomposition [J]. Journal of Geodesy, 2010, 84 (7): 449-456.

[19] AN Jiachun, NING Xinguo, WANG Zemin, et al. Antarctic ionospheric prediction based on spherical cap harmonic analysis and time series analysis [J]. Geomatics and Information Science of Wuhan University, 2015, 40 (5): 677-681.

[20] LIU Lilong, CHEN Jun, HUANG Liangke, et al. TEC forecast of short-term ionosphere based on wavelet-ARIMA [J]. Journal of Guilin University of Technology, 2016, 36 (2): 294-299.

[21] LU Chenlong, KUANG Cuilin, ZHANG Jinsheng, et al. Predicting ionosphere TEC with the combination of singular spectrum analysis and ARMA model[J]. Journal of Geodesy and Geodynamics, 2014,34(6): 44-49.

[22] TANG Jun, YAO Yibin, CHEN Peng, et al. Prediction models of ionospheric TEC improved by EMD method[J]. Geomatics and Information Science of Wuhan University, 2013, 38(4): 408-411, 444.

[23] WANG Ruopeng, ZHOU Chen, DENG Zhongxin, et al. Predicting f_0F_2 in the China region using the neural networks improved by the genetic algorithm[J]. Journal of Atmospheric and Solar-Terrestrial Physics, 2013, 92: 7-17.

[24] LIU J Y, CHEN C H, CHEN Y I, et al. A statistical study of ionospheric earthquake precursors monitored by using equatorial ionization anomaly of GPS TEC in Taiwan during 2001—2007[J]. Journal of Asian Earth Sciences, 2010, 39 (1-2): 76-80.

[25] CESARONI C, SPOGLI L, ARAGON-ANGEL A, et al. Neural network based model for global total electron content forecasting[J]. Journal of Space Weather and Space Climate, 2020, 10(S335): 11.

[26] ACHARYA R, ROY B, SIVARAMAN M R, et al. Prediction of ionospheric total electron content using adaptive neural network with in-situ learning algorithm[J]. Advances in Space Research, 2011, 47(1): 115-123.

[27] WANG Jianmin, HUANG Jiapeng, LIU Ziran, et al. Improvement of prediction model for ionospheric TEC with adaptive Kalman filter [J]. Journal of Navigation and Positioning, 2018, 6(2): 121-127.

[28] WANG Jianmin, HUANG Jiapeng, ZHU Huizhong, et al. Study of the ionosphere TEC forecasting method[J]. Science of Surveying and Mapping, 2016, 41(12): 47-52.

[29] HUANG Z, LI Q B, YUAN H. Forecasting of ionospheric vertical TEC 1-h ahead using a genetic algorithm and neural network[J]. Advances in Space Research, 2015, 55 (7): 1775-1783.

[30] SABZEHEE F, FARZANEH S, SHARIFI M A, et al. TEC regional modeling and prediction using ANN method and single frequency receiver over IRAN[J]. Annals of Geophysics, 2018, 61(1): GM103.

[31] TEBABAL A, RADICELLA S M, DAMTIE B, et al. Feed forward neural network based ionospheric model for the east African region [J]. Journal of Atmospheric and Solar-Terrestrial Physics, 2019, 191:105052.

[32] INYURT S, SEKERTEKIN A. Modeling and predicting seasonal ionospheric variations in Turkey using Artificial Neural Network (ANN)[J]. Astrophysics and Space Science, 2019, 364(4): 62.

[33] HUANG Guangbin, ZHOU Hongming, DING Xiaojian, et al. Extreme learning machine for regression and multiclass classification[J]. IEEE Transactions on Systems, Man,and Cybernetics, 2012, 42(2): 513-529.

[34] LI Lin, JI Hongbing. Signal feature extraction based on an improved EMD method [J]. Measurement, 2009, 42 (5): 796-803.

[35] WANG Tong, ZHANG Mingcai, YU Qihao, et al. Comparing the applications of EMD and EEMD on time-frequency analysis of seismic signal[J]. Journal of Applied Geophysics, 2012, 83: 29-34.

[36] SU Wenbin, LEI Zhufeng. Mold-level prediction based on long short-term memory model and multi-mode decomposition with mutual information entropy[J]. Advances in Mechanical Engineering, 2019, 11(12): 168.

[37] JIN Xuebo, YANG Nianxiang, WANG Xiaoyi, et al. Hybrid

deep learning predictor for smart agriculture sensing based on empirical mode decomposition and gated recurrent unit group model[J]. Sensors, 2020, 20(5): 1334.

[38] ZHANG Qian, ZHANG Jinjin. Short-term load forecasting method based on EWT and IDBSCAN[J]. Journal of Electrical Engineering & Technology, 2020, 15(2): 635-644.

[39] CHEN Weijie, GIGER M L, BICK U. A fuzzy C-means-based approach for computerized segmentation of breast lesions in dynamic contrast-enhanced MR images[J]. Academic Radiology, 2006, 13(1): 63-72.

[40] CHIN C S, JI Xi, WOO W L, et al. Modified multiple generalized regression neural network models using fuzzy C-means with principal component analysis for noise prediction of offshore platform [J]. Neural Computing and Applications, 2019, 34(4): 1127-1142.

[41] KELOTRA A, PANDEY P. Stock market prediction using optimized deep-ConvLSTM model[J]. Big Data, 2020, 8(1): 5-24.

[42] HATHAWAY R J, BEZDEK J C. Fuzzy C-means clustering of incomplete data[J]. IEEE Transactions on Systems, Man, and Cybernetics, Part B, 2001, 31(5): 735-744.

[43] YU Jian, CHENG Qiansheng, HUANG Houkan. Analysis of the weighting exponent in the FCM[J]. IEEE Transactions on Systems, Man, and Cybernetics, Part B, 2004, 34(1): 634-639.

[44] GHOSH S, KUMAR S. Comparative analysis of k-means and fuzzy C-means algorithms[J]. International Journal of Advanced Computer Science and Applications, 2013, 4(4): 35-39.

[45] YIN Dongyang, SHENG Yifa, JIANG Mingjie, et al. Short-term wind speed forecasting using Elman neural network based on rough set theory and principal components analysis[J]. Power System Protection and Control, 2014, 42(11): 46-51.

[46] SUN Zhenli, WANG Han, LAU W S, et al. Application of BW-ELM model on traffic sign recognition[J]. Neurocomputing, 2014, 128: 153-159.

[47] HUANG Guangbin, ZHU Qinyu, SIEW C K. Extreme learning machine: theory and applications [J]. Neurocomputing, 2006, 70(1-3): 489-501.